ELSEVIER

Cardiovascular Research 42 (1999) 490–502

Cardiovascular Research

β-adrenergic action on wild-type and KPQ mutant human cardiac Na^+ channels: shift in gating but no change in Ca^{2+}: Na^+ selectivity

Rashmi Chandra[a], Vijay S. Chauhan[a], C. Frank Starmer[b], Augustus O. Grant[a,*]

[a]*Duke University Medical Center, Durham, NC, USA*
[b]*Medical University of South Carolina, Charleston, SC, USA*

Received 14 October 1998; accepted 11 January 1999

Abstract

Objective: Prior studies of the modulation of the Na^+ current by sympathetic stimulation have yielded controversial results. Separation of the Na^+ and Ca^{2+} currents poses a problem in myocyte preparations. The gating of cloned Na^+ channels is different in oocytes compared with mammalian expression systems. We have examined the sympathetic modulation of the α-subunit of the wild-type human cardiac Na^+ channel (hH1) and the long QT-associated mutant, ΔKPQ, expressed in human embryonic kidney cells. **Methods:** Stable cell lines of hH1 and ΔKPQ were established in human embryonic kidney cells. Whole-cell and single-channel currents were measured with the patch–clamp technique. Sympathetic stimulation was effected by exposure to isoproterenol or 8-bromo-cAMP. Na^+ channel activation and inactivation were determined using standard voltage clamp protocols. Ca^{2+}: Na^+ permeability ratio was determined under bi-ionic conditions. **Results:** We observed a qualitatively different effect of sympathetic stimulation on the cardiac Na^+ current from that reported in frog oocytes: activation and inactivation kinetics were shifted to more negative potentials. This shift was similar for both hH1 and ΔKPQ. [$\Delta V_{0.5}$ for inactivation: 8.3±1.7 mV, $p<0.001$ (hH1); 6.8±0.9 mV, $p<0.001$ (ΔKPQ)]. Increased rate of closed-state inactivation contributed to the shifting of the inactivation–voltage relationship. Open-state inactivation was not affected as mean open times were unchanged. Reversal potential measurement in hH1 suggested a low Ca^{2+}: Na^+ permeability ratio of 0.017, uninfluenced by sympathetic stimulation. In ΔKPQ, the size of the persistent relative to the peak current was increased with 8-bromo-cAMP from 3.0±0.7% to 4.3±0.6% ($p=0.056$). **Conclusions:** Sympathetic stimulation exerts multiple effects on the gating of hH1. Similar effects are also seen in ΔKPQ which may increase arrhythmia susceptibility in long QT syndrome by modifying the Na^+ channel contribution to the action potential.

Keywords: Na-channel; Long QT syndrome; Adrenergic agonists; Single-channel currents; Membrane permeability

1. Introduction

The sympathetic nervous system plays an important role in the genesis of a variety of ventricular arrhythmias [1,2]. β-adrenergic blockade improves survival in the common form of ventricular tachycardia associated with coronary artery disease and cardiomyopathy [3]. A childhood form of polymorphic ventricular tachycardia is precipitated by stress, exercise and isoproterenol infusion, and is prevented by β-adrenergic blockade [4]. An important role of the sympathetic nervous system has also been apparent in the congenital long QT syndrome (LQTS) [5–7]. QT interval prolongation, T-wave alternans and attacks of torsade de pointes are often precipitated by exercise and fright [8]. Some patients may have a normal QT interval at rest, but demonstrate marked QT prolongation and ventricular arrhythmias during exercise [9,10]. A number of investigators have demonstrated the benefit of anti-adrenergic treatments in the LQTS [6,11].

Disturbances in the properties of ion channels that generate the action potential play an important role in the genesis of arrhythmias. Since the sodium channel sustains propagation in the atrial and ventricular myocardium and the ventricular conduction system, it is likely to be crucial

*Corresponding author. Tel.: +1-919-684-3901; fax: +1-919-681-8978.

E-mail address: aog@carlin.mc.duke.edu (A.O. Grant)

Time for primary review 26 days.

0008-6363/99/$ – see front matter
PII: S0008-6363(99)00042-5

in the genesis of arrhythmias. The influence of adrenergic stimulation of the sodium current is controversial. In multicellular preparations and isolated myocytes, the most commonly observed effect is a shift of the inactivation membrane–voltage relationship to more negative potentials [12–17]. Recently, Santana et al. have described a novel mechanism of modulation of cardiac sodium channels by β-adrenergic stimulation: the induction of a 'slip-mode conductance' in which the calcium to sodium permeability ratio of the sodium channel is increased from approximately zero to 1.25 during isoproterenol exposure [18]. This is a surprising result as calcium ions have been reported to block the sodium channel [19,20]. Sodium channels exhibit permeability to calcium only under special circumstances [21–23]. A major difficulty with those experiments is separation of a significant calcium current from the sodium current. The action of drugs e.g., the organic Ca^{2+} blockers that are used to separate the calcium and sodium currents are reversed by sympathetic stimulation [24–26].

The cloning of the gene encoding the cardiac sodium channel provided a potentially simple system to analyze adrenergic modulation of the sodium channel [27,28]. The effects of the sympathetic stimulation on the LQTS-associated sodium channel mutations could also be directly examined. Of the many LQTS-associated sodium channel mutations that have been recently described, that associated with the nine base pair deletion, ΔKPQ is the most severe [29–33]. The site of the deletion involves a consensus site for phosphorylation of the sodium channel. Therefore, it would be of interest to determine the influence of sympathetic stimulation on the gating kinetics and the late component of the sodium current expressed by this mutant sodium channel. Scheibmayer and colleagues observed a qualitatively different effect of sympathetic stimulation when the wild-type sodium channel is expressed in frog oocytes compared with that observed in native cell membranes [34]. Current amplitude is increased by 30–40% with no shift in activation or inactivation kinetics. It is not clear if the increase in current amplitude is a property of the human cardiac sodium channel or of the oocyte expression system. With regard to the adrenergic-induced change in cation selectivity, the oocyte expression system is not optimal for re-examination of this issue because the intracellular concentration of ions is difficult to control.

We have examined the effects of β-adrenergic stimulation on the wild-type and LQTS-associated sodium channel mutation, ΔKPQ, in a mammalian expression system using whole-cell and single-channel recordings. Experiments with the wild-type channel offered the opportunity to resolve the action of β-adrenergic stimulation on the human cardiac sodium channel in a mammalian system expressing a single isoform. Human embryonic kidney (HEK) cells express an endogenous β-adrenergic receptor that can be readily stimulated by isoproterenol [35]. We also confirmed the effects reported here when the β-adrenergic receptor was bypassed by exposing the HEK cells to 8-bromo-cAMP (8BcAMP), a membrane permeable analogue of cAMP. The predominant effect of β-adrenergic stimulation under our recording conditions was a shift of the inactivation and to a lesser extent, the activation membrane–voltage relationship to more negative potentials. An increase in the rate of closed-state inactivation contributed to the negative shift. Single-channel open time was not affected, suggesting no influence on open-state inactivation. With the same intra- and extracellular sodium concentration, the sodium current reversed at the same potential during the control and exposure to isoproterenol. Further, the reversal potential shifted to more negative potentials when external sodium ions were withdrawn during isoproterenol exposure.

The relative amplitude of the slow component of the sodium current for the ΔKPQ mutant channel was increased as it did not demonstrate the β-adrenergic enhancement of inactivation. The implications of this effect will depend on the effects of β-adrenergic stimulation on the other ion currents that contribute to repolarization.

2. Methods

The experiments were performed on HEK cells expressing the α-subunit of the wild-type sodium channel (hH1) or the ΔKPQ mutant sodium channel in which nine base pairs have been deleted from the linker between domains three and four. The techniques for establishing the cell lines have been described in detail previously [36]. *hH1* was cloned into the plasmid pREP4 and 293-EBNA cells transfected with pREP4/*hH1* using lipofectamine (GIBCO-BRL, Gaithersburg, MD). Stable transfectants were selected by culturing the cells in media containing 500 μg/ml of hygromycin (Boehringer Mannheim, Indianapolis, IN). The ΔKPQ mutation was confirmed by direct sequencing and the mutant cloned into pcDNA3. HEK-293 cells were transfected with pcDNA3/ΔKPQ using lipofectamine. The stable transfectants were selected by culture in medium containing 500 μg/ml G418 (GIBCO-BRL). These stable cell lines have been established for over two years and continue to express robust Na^+ currents.

2.1. Experimental set-up

For most of the whole-cell recordings, cells were superfused with Na^+ external solution; micropipettes were filled with cesium internal solution. The cesium ions blocked the endogenous K^+ currents present in these cells [37]. Under these recording conditions, the Na^+ current was the only measurable ionic current. For single-channel recordings, the cells were perfused with a high potassium solution that reduced the membrane potential to zero mV.

Membrane potential in cell-attached patches is quoted as absolute values.

We assessed the stability of the gating kinetics of the sodium current in the HEK cells by performing control whole-cell voltage clamp experiments. Voltage–clamp protocols were performed at baseline and then after 7.5 min of drug-free perfusion. In separate experiments, voltage–clamp protocols were applied at baseline and then repeated during 3 min of superfusion with external solution containing 1 μM isoproterenol or 5 mM 8BcAMP. For the single-channel experiments, control data were acquired 10 min after giga ohm seal formation. Cells were then exposed to the drug for 3 min and the protocol repeated. The whole-cell and single-channel data reported in this manuscript were obtained during continuous recording from the same cell or patch.

The solutions used in the electrophysiology experiments had the following composition (mM): Na^+ external solution: NaCl 130, KCl 4, $CaCl_2$ 1, $MgCl_2$ 5, HEPES 5 glucose 5 (pH 7.4 with NaOH); Low Na^+ external solution: NaCl 10, CsCl 120, KCl 4, $CaCl_2$ 2, $MgCl_2$ 1, HEPES 5, Glucose 5 (pH 7.4 with CsOH); Cs^+ micropipette solution: CsCl 130, $MgCl_2$ 1, Mg ATP 5, BAPTA 10, HEPES 10 (pH 7.2 with CsOH); Cesium/Na^+ micropipette solution was similar to the Cs^+ micropipette solution, but CsCl was reduced to 120 mM and [Na^+] was 10 mM; *N*-methyl-D-glucamine (NMG) external solution: NMG 150, $CaCl_2$ 2, HEPES 5, glucose 5 (pH 7.4 with HCl); NMG micropipette solution: NMG 140, NaCl 10, Mg ATP 5, HEPES 5 and EGTA 5 (pH 7.2 with HCl); high K^+ external solution: K-aspartate 140, KCl 10, $MgCl_2$ 2, $CaCl_2$ 1, glucose 5, HEPES 5 (pH 7.4 with KOH); Na^+ micropipette solution: NaCl 140, KCl 5, $MgCl_2$ 2.5, $CaCl_2$ 0.5, HEPES 5 (pH 7.4 with NaOH). All experiments were performed at room temperature (20–22°C). Isoproterenol and 8BcAMP were obtained from Sigma Chemical.

2.2. Recording techniques

Whole-cell and single-channel currents were recorded with a Dagan 3900A integrating- or EPC-7 patch–clamp amplifier (Dagan, Minneapolis, MN; Adams and List, NY). Whole-cell currents were recorded with 0.5–1.0-MΩ microelectrodes. A silver/silver wire coupled each microelectrode to the input of the amplifier. A similar wire embedded in agar/micropipette solution formed the bath reference. Series resistance was compensated using conventional and supercharging techniques. At the beginning of each whole-cell experiment, adequacy of voltage control was assessed as previously described [38]. For all the whole-cell experiments, the potential was set at −100 mV. Stable recordings could not be obtained if these cells were held at more hyperpolarized potentials for prolonged periods. The current–voltage relationship was determined with 20-ms pulses of increasing amplitude applied at 1000-ms intervals. The pulse amplitude was incremented in 5-mV steps. The steady-state inactivation curve was determined by the application of 500-ms prepulses from −130 to −55 mV. A 20-ms test pulse to −20 mV followed each prepulse. The prepulse potential was incremented in 5-mV steps. The development of inactivation was determined at −80 mV by the application of prepulses of increasing duration to that potential followed by test pulses to −20 mV. The magnitude of the late component of Na^+ current was determined using a voltage ramp with a slope of 100 mV/s. Whole-cell currents were filtered at 10 kHz and digitized at 40 kHz.

Single Na^+ channel currents were recorded with 5−10-MΩ microelectrodes [39]. The holding potential was set between −90 and −75 mV. Test pulses of 200 ms were applied to various potentials. Currents were filtered at 2.5 kHz and digitized at 20 kHz.

2.3. Data analysis

The analysis of whole-cell and single-channel currents has been described in prior studies from this laboratory [38,39]. Peak currents were measured with custom software written in C programming language. Activation and inactivation curves were fit with a Boltzman function using a Marquardt routine:

$$y = 1/(1 + \exp[V - V_{0.5}]/k)$$

where y is the activation or inactivation variable; V is the membrane potential, $V_{0.5}$ the potential at which $y = 0.5$ and k the slope factor. The time constant, τ, for the development of inactivation was obtained from the following equation:

$$I_t = \sum I_o \exp(-t/\tau)$$

where I_t is the test pulse current at prepulse duration t and I_o the current at −20 mV in the absence of the inactivating prepulse.

An automatic detection scheme with the threshold set at 0.5 was used to detect single openings in leakage- and capacity subtracted currents. Open time histograms were fit with a single exponential using a least square procedure. The accuracy of this approach has been documented using simulated data from a gating model using known rate constants [40]. Data are quoted as mean±SEM. Comparisons of data obtained from the same cell or patch were made with a paired t-test. Other comparisons were made with an unpaired t-test and $p < 0.05$ was considered significant.

3. Results

3.1. Characterization of the transient inward current

First, we demonstrate that the transient sodium current is the only significant inward current recorded from the

stably transfected HEK cells under our recording conditions. Membrane current–voltage relationships were determined by applying 20-ms pulses, incremented in 5-mV steps, from a holding potential of −100 mV. Illustrative currents in response to voltage steps to −60, −40, −20, 0 and +20 in a cell expressing the wild-type sodium current are shown in panel A of Fig. 1. The peak inward current of 5 nA was observed at −20 mV. Current recorded from the same cell during exposure to 60 μM tetrodotoxin are shown in panel B. Tetrodotoxin blocked the transient inward current. Superfusion of the cell with tetrodotoxin-free solution partially reversed the current block. Blockade of the inward current by TTX was demonstrated in four cells. The transfected cells therefore express a tetrodotoxin-susceptible inward current. The concentration of TTX required for current blockade placed the channels in the TTX-resistant class [41]. Next, we show that the inward current is carried by sodium ions. Panel D shows inward currents recorded from another cell with the current–voltage relationship protocol. A peak inward current of 7.1 nA was observed at a test potential of 0 mV. The external solution was switched to a solution in which sodium ions were replaced by the impermeant organic cation NMG (NMG external solution). All transient inward currents were abolished by NMG. Similar results were obtained in five cells. We conclude that the only significant transient inward current was blocked by tetrodotoxin and carried by sodium ions.

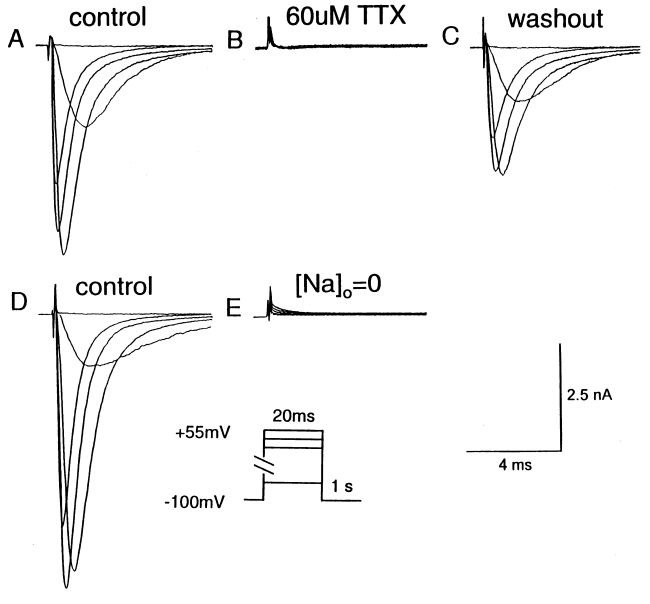

Fig. 1. Currents expressed by transfected cells are blocked by tetrodotoxin and carried by sodium ions. Whole-cell currents recorded from a cell expressing hH1 were elicited by voltage clamp pulses from a holding potential of −100 mV and test pulses incremented in 5-mV steps. Panel A shows currents recorded at test potentials of −60, −40, −20, 0, and +20 mV with normal external Na solution. Panel B shows currents recorded with the sample pulse protocol during superfusion of the cell with a solution containing 60 μM tetrodotoxin. The transient inward current is blocked by tetrodotoxin. After washing for 3 min with a drug-free solution, the blockade is partially reversed. Panel D and E show currents recorded from a different cell using the same voltage clamp protocol. The data in panel D were obtained during superfusion with normal sodium external solution; the data in panel E were obtained during superfusion with NMG external solution. The small initial spikes in all current tracings are capacitance transients.

3.2. β-Adrenergic modulation of sodium channel

In native cells, the voltage dependence of the gating kinetics of the sodium current shifts to more negative potentials during conventional whole-cell recordings [38,42]. We examined the stability of the activation and inactivation kinetics of hH1 and ΔKPQ expressed in HEK cells. Over a 7.5-min drug-free perfusion period, we observed no change in the mid-point or slope factor of the activation or inactivation curves. These results are included in the summary data presented below.

The effects of a 3-min exposure to 5 mM 8BcAMP on the activation and inactivation of hH1 are illustrated in Fig. 2. Under control conditions, the threshold for current activation was −60 mV and a peak current of −5.7 nA was observed at −10 mV. The half potential for activation was −29.8 mV. During exposure to 8BcAMP peak sodium current decreased to −4.6 nA and was observed at −15 mV. The activation curve was shifted to more negative potentials ($V_{0.5}$ −35.7 mV) such that larger currents were observed at some potentials on the negative limb of the current–voltage relationship. The reduction in peak sodium current resulted from a negative shift in the half potential for inactivation from −84.2 to −92.2 mV with 8BcAMP (Fig. 2). The average shifts in half potential for activation and inactivation with 8BcAMP and 1 μM isoproterenol are presented in Fig. 3.

For ΔKPQ, both 5 mM 8BcAMP and 1 μM isoproterenol reduced the peak current and shifted the potential for half activation and inactivation to more negative potentials ($p<0.05$). When the magnitude of shifts observed with hH1 and ΔKPQ were compared, there was a trend toward a smaller shift with ΔKPQ, however the differences were not statistically significant. For both channel types, the negative shifts of the inactivation voltage relationship were significantly larger than the shifts of the activation voltage relationship. We also performed a limited number of experiments with lower concentrations of 8BcAMP (500 μM, $n=4$) and isoproterenol (100 nM, $n=4$) in cells expressing hH1. Similar shifts in gating were observed at the lower concentrations of both drugs.

The negative shift in inactivation may result from an acceleration of the rate of closed- and open-channel inactivation. We examined the former possibility by determining the rate of closed-channel inactivation using whole-cell recordings. Peak current during a test pulse to −20 mV was measured following conditioning pulses of increasing duration to −80 mV. As illustrated in Fig. 4, peak test-pulse current declined as the duration of the conditioning pulse was increased. Test-pulse current de-

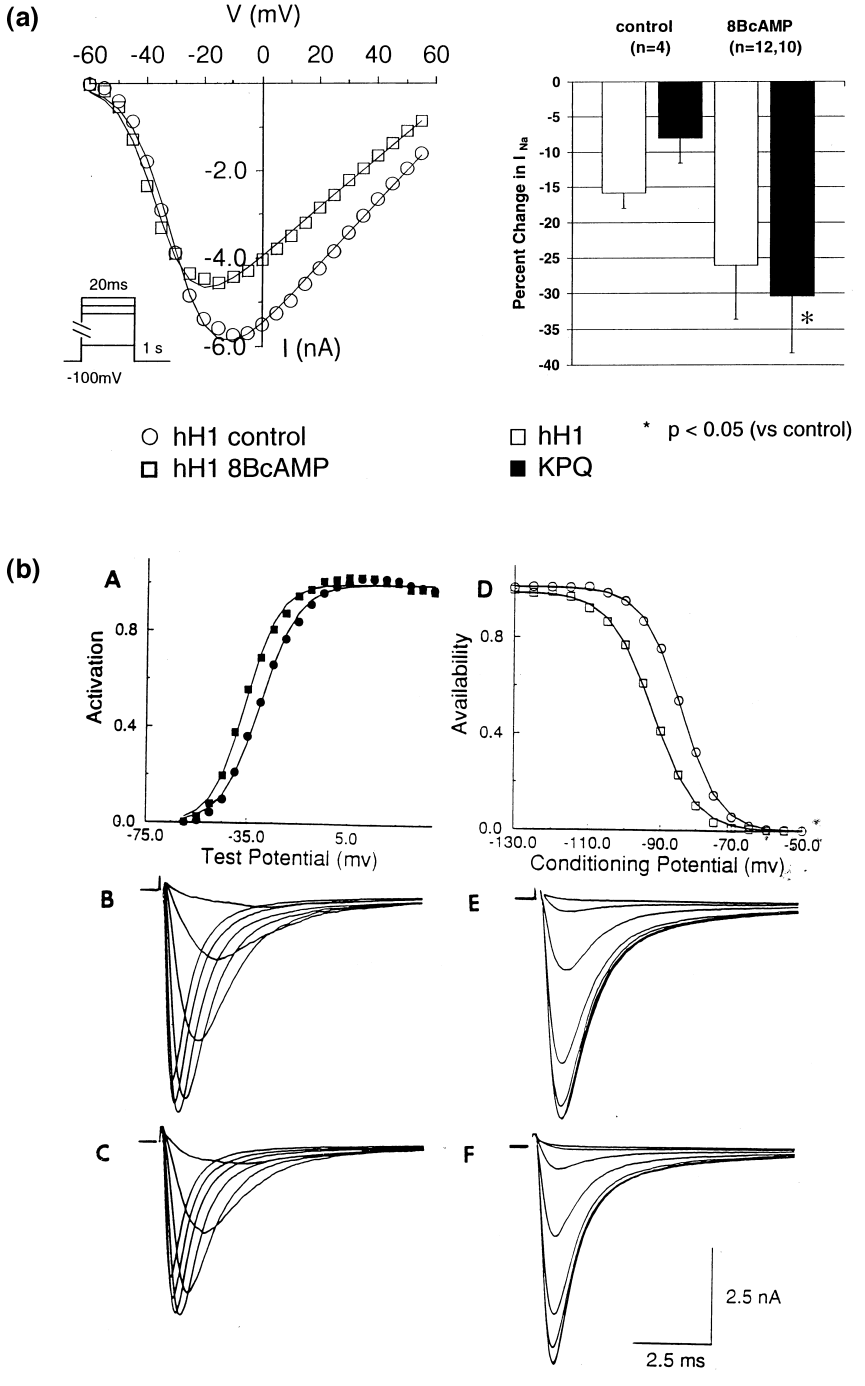

Fig. 2. (a) Change in the current–voltage relationship of hH1 by 8BcAMP. The panel on the left shows the reduction in peak sodium current during exposure to 8BcAMP (square) compared to the control (circle) in a cell expressing hH1. The right panel summarizes the percent reduction in peak sodium current with 8BcAMP for both hH1 and ΔKPQ. The change in peak sodium currents seen in the control cells were assessed over a 7.5 min drug-free perfusion period; (b) Hyperpolarizing shifts of activation and inactivation gating by 8BcAMP. Panels A–C show the effect of 8BcAMP on activation. The activation curve during the control (closed circles) is shifted to a more negative potential during exposure to 8BcAMP (closed squares). The parameters are: $V_{0.5}$ of −29.8 mV and a slope factor, k of 7.5 mV during the control and −35.7 and 6.7 during exposure to 8BcAMP. Representative original current traces are shown in panels B (control) and C (during exposure to 8BcAMP). The holding potential was −100 mV and the test potential incremented in 5-mV steps. Currents to −50, −40, −30, −20, −10, 0 and 10 mV are shown in panel B. The inactivation curves in panel D had parameters of $V_{0.5}$ of −84.2 mV and k of 5.4 mV during the control (open circles) and −92.2 mV and 6 mV during exposure to 8BcAMP (open square). The currents in panels E (control) and F (8BcAMP) obtained at a test potential of −20 mV after conditioning steps from −130 to −60 in 10-mV increments are shown.

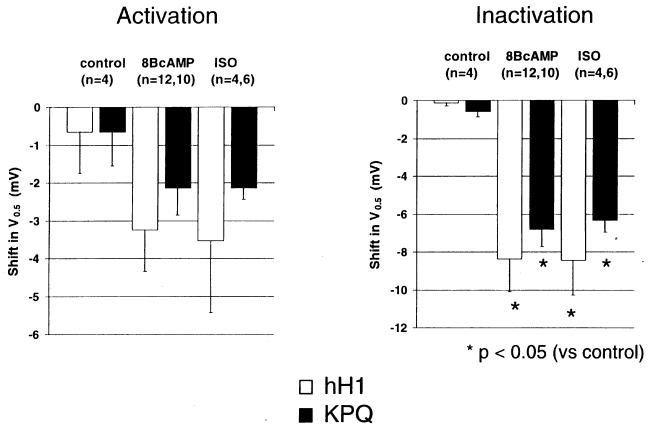

Fig. 3. Summary of the shifts of the voltage dependence of activation and inactivation during the control and exposure to 1 μM isoproterenol and 5 mM 8BcAMP. Shifts in half potential for activation are shown in the left panel; those for inactivation are shown in the right panel. The kinetic shifts seen in control cells were assessed over a 7.5-min drug-free perfusion period.

clined faster during exposure to 5 mM 8BcAMP compared to the control. During the control and 8BcAMP exposure, the data fit well with a biexponential function. The time constants were 28 and 111 ms during the control and 24 and 90 ms exposure to 8BcAMP. In other experiments, the data fit adequately with a single exponential. Therefore, we used the half times for the decline of the current during the test pulse to compare the kinetics of closed-channel inactivation in all cells. The half-time for the development of inactivation ($T_{0.5}$) decreased from a control value of 55±9 ms to 32±5 ms ($n=4$, $p<0.05$) during exposure to 8BcAMP in cells expressing hH1. In the case of ΔKPQ, closed-channel inactivation also developed faster with β-adrenergic stimulation ($T_{0.5}$ 14±1 ms, control; $T_{0.5}$ 11±1 ms, 1 μM isoproterenol; $n=4$, $p<0.05$). When compared to hH1, ΔKPQ showed faster kinetics of closed-channel inactivation under control and β-adrenergic stimulation.

We compared the rate of open-state inactivation during control and exposure to isoproterenol in cell-attached patches in HEK cells expressing hH1 or ΔKPQ. For both cell types, the density of the channels was sufficiently high that moderate reductions of membrane potentials were used to limit the extent of overlapping events. If the reductions in membrane potential were sufficiently large to observe almost exclusively non-overlapping events, during adrenergic stimulation too few events were available for analysis. Fig. 5 illustrates membrane currents in a cell-attached patch from a cell expressing hH1. The holding potential was set at −90 mV and depolarizing trials were performed to −40 and −30 mV. Each panel shows currents during five consecutive trials, and the ensemble average current from 100 trials. The average current showed the expected increase in amplitude and relaxation kinetics with depolarization. Mean channel open time was 0.8 ms at −40 mV and 0.9 ms at −30 mV. During exposure to isoproterenol, there was little change in the

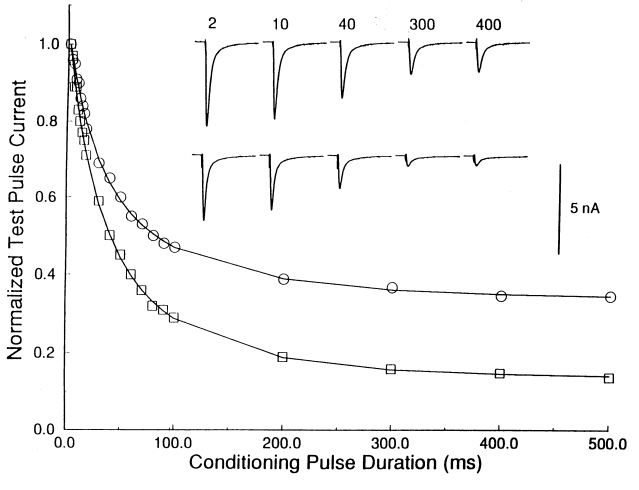

Fig. 4. Kinetics of the development of closed-state inactivation. Sodium currents were elicited by 20-ms voltage steps to −20 mV after conditioning pulses of increasing duration to −80 mV. Test pulse peak currents have been normalized and plotted against the conditioning pulse duration. Data obtained during the control (circles) and exposure to 5 mM 8BcAMP (squares) were fitted with two exponentials. The time constants were 28 and 111 ms during the control and 24 and 90 ms during exposure to 5 mM of 8BcAMP. The insert shows representative currents obtained at the indicated conditioning durations; upper group, controls; lower group, 8BcAMP.

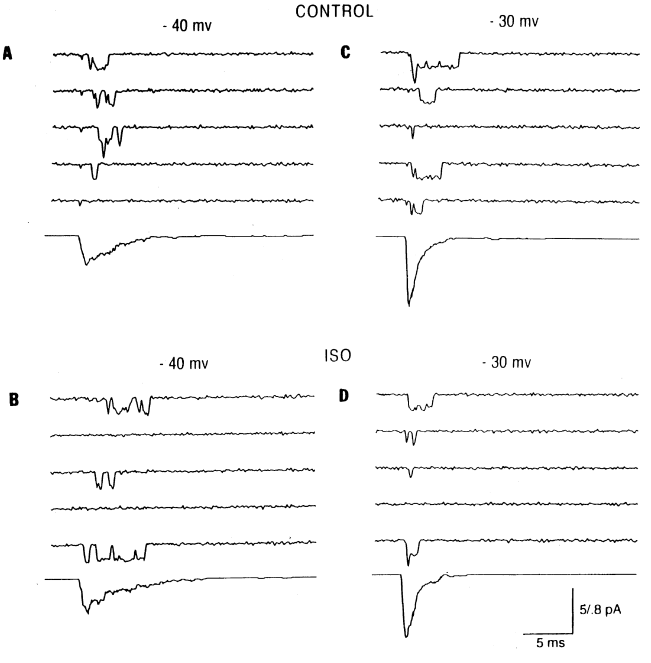

Fig. 5. Effects of isoproterenol on single sodium channel currents recorded in the cell-attached configuration from cells expressing hH1. Each panel shows currents during five consecutive depolarizing trials and the average current (lowest tracing) obtained by summing 100 trials. Current shown in panels A and C were obtained during the control at test potentials of −40 and −30 mV. Currents in panels B and D were obtained during exposure to 1 μM isoproterenol at test potentials of −40 and −30 mV. The holding potential was −90 mV throughout all four sets of recordings.

peak average current at −40 and −30 mV. This result is consistent with the opposing influences of the negative activation shift and more steady-state inactivation during β-adrenergic stimulation observed with the whole-cell recordings. The single-channel current amplitude was unchanged during isoproterenol exposure, 2.00 pA at −40 mV and 1.85 pA at −30 mV. This suggests that isoproterenol does not change the field sensed by the ion channel. Mean open times were 0.80 and 0.82 ms at −40 and −30 mV during adrenergic stimulation. The mean values from three experiments were 0.8±0.2 and 0.7±0.1 ms during the control and during exposure to isoproterenol at −40 mV and 0.80±0.07 and 0.80±0.03 at −30 mV.

When the holding potential was sufficiently reduced to result in a decrease in the average current during exposure to isoproterenol, there was also no reduction in mean open time. This is illustrated by an experiment with the ΔKPQ mutant in Fig. 6. The holding potential was −80 mV and the test potential was −30 mV. The peak average current decreased by 66% during exposure to isoproterenol. In this experiment, the mean open time was 0.6±0.6 ms during the control and 0.5±0.5 ms during exposure to isoproterenol. The decrease in average current could largely be accounted for by an increase in the probability of closed-state inactivation, 0.43 during the control and 0.63 during exposure to isoproterenol. This is consistent with the whole-cell experiments showing an increase in rate of closed-state inactivation.

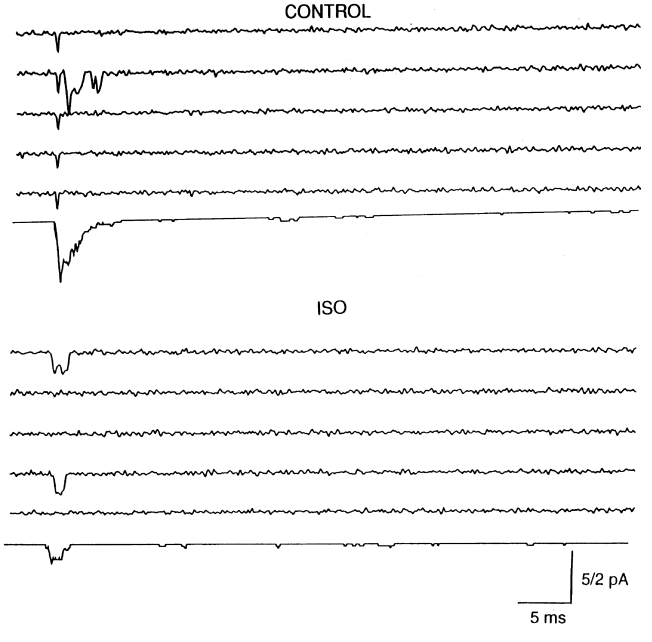

Fig. 6. Effect of isoproterenol on single sodium channel currents recorded in the cell-attached configuration from cells expressing ΔKPQ. The upper panel shows five consecutive current responses to test pulses to −30 mV and the current obtained by averaging 100 such responses (lowest tracing) during the control. The lower panel shows data obtained during exposure to 1 μM isoproterenol at a test potential of −30 mV. The holding potential was −80 mV throughout both sets of recordings.

3.3. Effects of adrenergic activation on calcium permeability of the sodium channel

The expression of the human cardiac sodium channel in human embryonic kidney cells provided a simpler system to examine the calcium to sodium permeability ratio from reversal potential measurements. In the human embryonic kidney cells, the transfected human cardiac sodium channel is the only transient current expressed. Therefore, blockers to separate the calcium and sodium currents were not required. We used several approaches to determine whether the calcium permeability was influenced by sympathetic stimulation. These experiments were performed in the cells expressing the wild-type sodium channel. For the initial set of experiments, we used equal sodium concentrations of 10 mM in the intra- and extracellular solutions ($[Cs]_o = [Cs]_i = 120$ mM). An experiment showing the current–voltage relationships and membrane currents are illustrated in Fig. 7. During control and exposure to isoproterenol, the reversal potential was −1 and −2.5 mV, respectively. Mean values in four experiments were −2.2±0.6 mV during the control and −3±1 mV during exposure to isoproterenol. Since there is no significant change in reversal potential, we conclude that the Na^+ to Ca^{2+} permeability ratio of the channel is unchanged.

To further examine the effects of β-adrenergic stimulation on the calcium conductance of the sodium channel, we examined the current–voltage relationship as $[Na^+]_o$ was varied during continued exposure to isoproterenol. If isoproterenol increased the calcium permeability of the sodium channel, one would expect a positive shift of the reversal potential when $[Na^+]_o$ is reduced. Fig. 8 illustrates an experiment in which $[Na^+]_o$ was varied during exposure to isoproterenol. With the same intra− and extracellular sodium concentration of 10 mM, the reversal potential was −1.5 mV during the control and −3.1 mV during isoproterenol exposure. On withdrawal of external Na^+, the reversal potential shifted to −25.3 mV. The shift is highlighted in the actual currents illustrated in panels A–C of Fig. 8. The filled arrows denote the current at a test potential of −15 mV: −0.57, −0.51 and +0.2 nA during the control, exposure to isoproterenol, and Na^+ withdrawal during the continued presence of isoproterenol. The inward current that was not completely abolished with $[Na]_o$ 0 mM (panel C) which is unlikely to be carried by Ca^{2+} since the reversal potential did not shift positively towards E_{Ca}. Rather, this may be a small potassium current since the p_K/p_{Na} is similar to the p_{Ca}/p_{Na} under basal conditions. In an additional five cells, 1 μM isoproterenol was added after sodium currents had been eliminated in the presence of $[Na]_o$ 20 μM. The $[Ca^{2+}]_o$ was fixed at 2 mM. We observed no increase in inward sodium current during isoproterenol application (data not shown).

Permeability ratio of ion pairs for a given ion channel can be most simply determined by reversal potential

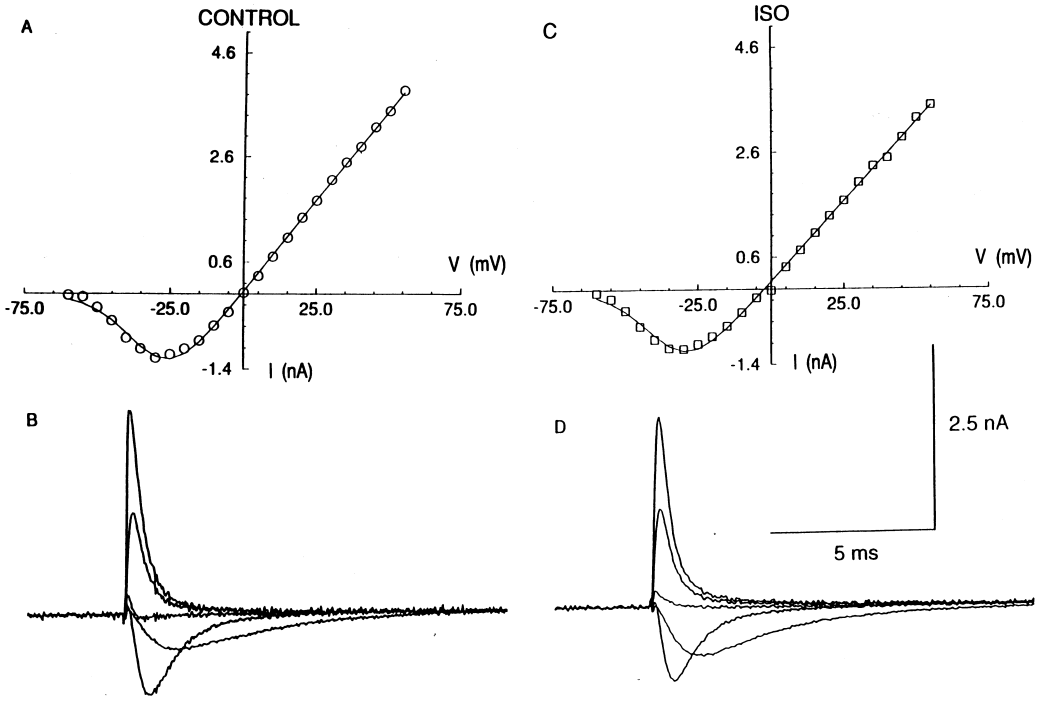

Fig. 7. Effects of isoproterenol on the current–voltage relationship of hH1. Panels A and C show peak currents as a function of the test potential as voltage steps of increasing amplitude were applied from a holding potential of −100 mV during the control (open circles) and exposure to 1 μM isoproterenol (squares). Representative membrane currents observed at test potentials of −45, −25, 0, +30 and +40 mV are shown in panels B and D. The intra- and extracellular sodium concentrations were 10 mM; the extracellular calcium concentration was 2 mM.

measurements under bi-ionic conditions [43]. We approximated this condition by using an external solution with 150 mM NMG, [Ca^{2+}] 2 mM and a micropipette solution of 140 mM NMG, [Na^{+}] 10. The sodium channel is assumed to be impermeable to the large organic cation NMG [44]. Illustrative currents at test potentials of −60, +10 and +55 mV during determination of membrane current–voltage relationships are shown in panel A of Fig. 9. At no test potential was an inward current observed. Panel B illustrates the membrane current at the same test potentials during exposure to isoproterenol. Again, all currents were outward. The membrane current in four cells were normalized by the peak current at a test potential of +55 mV and plotted against the test potential in panel C. There was no significant difference in the extrapolated reversal potential during the control and exposure to isoproterenol. The calcium: sodium permeability ratio was calculated using the Fat and Ginsberg modification of the constant field equation [45]:

$$E_{rev} = RT/2F \ln 4 P_{Ca} [Ca^{2+}]_o / P_{Na} [Na^{+}]_i$$

where E_{rev}, is the reversal potential, R, T and F have their usual meanings, P_{Ca} the calcium permeability and P_{Na} the sodium permeability. The estimated P_{Ca}/P_{Na} during the control and exposure to isoproterenol was 0.017. We conclude that in this simplified cell system, the sodium channel has no significant permeability to calcium ions even during exposure to isoproterenol.

3.4. Effect of adrenergic activation on the late persistent sodium current

A characteristic feature of the ΔKPQ mutant sodium channel is the frequent entry into gating modes where the channel either fails to inactivate or returns to the open state after initial fast inactivation [31,32]. This results in a persistent component of inward current at depolarized potentials. The size of this component of current can be efficiently analyzed by the application of slow voltage ramps in the whole-cell configuration [46,47]. If the voltage ramp is sufficiently slow, channels will undergo fast inactivation and the persistent current will be evident as a non-linearity in the current response. We used a ramp with a slope of 100 mV/s to examine the persistent current during the control and exposure to isoproterenol.

Fig. 10 illustrates the ramp response and step current–voltage relation in a cell expressing the ΔKPQ mutant. Because of the small magnitude of the persistent currents, they had to be recorded at high gain. The peak value of the persistent current was 124 pA during the control and 119 pA during exposure to 5 mM 8BcAMP. However, the step current–voltage peak decreased from −5.2 to −2.4 nA. Therefore, as a fraction of the peak current, the persistent current is larger during exposure to isoproterenol. In five experiments, the peak ramp current was 3.0±0.7% of the peak current during the control and 4.3±0.6% during exposure to isoproterenol ($p = 0.056$).

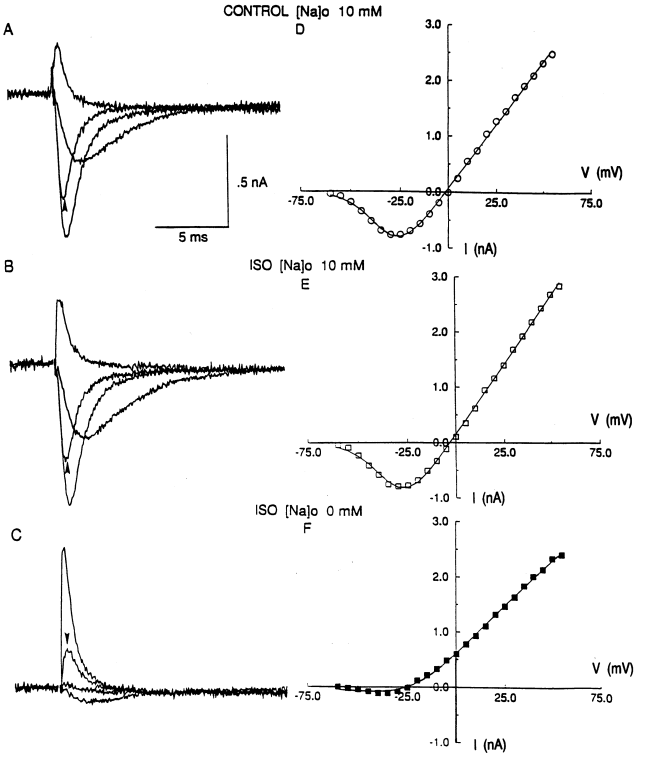

Fig. 8. The influence of withdrawal of external sodium on the membrane current during exposure to isoproterenol. Current–voltage relationships were determined during the control, exposure to 1 μM isoproterenol, and during withdrawal of extracellular sodium in the continued presence of isoproterenol. The holding potential was −100 mV. Membrane currents observed at the test potential of −45, −25, −15 and +5 mV are shown in panel A–C. In each panel, the arrow indicates the current recorded at a test potential of −15 mV. In panels A and B, the current at −15 mV is inwards whereas in the C it is outwards, signifying a negative shift in the reversal potential of the sodium current. Overall peak current–voltage relationships are shown in panels D–F.

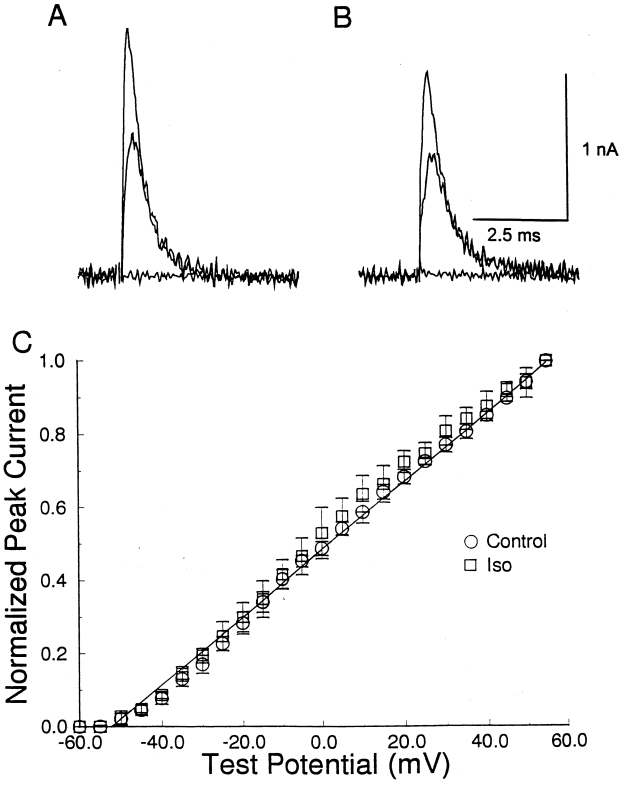

Fig. 9. Influence of isoproterenol on sodium channel permeability under bi-ionic conditions. Whole cell sodium currents were recorded from cells expressing hH1 using the Ca–NMG external solution and Na–NMG internal solution. Illustrative currents at test potentials of −60, +10, and +55 mV during the control and exposure to 1 μM isoproterenol are shown in panels A and B respectively. Average data from four cells are presented in panel C. The error bars represent the standard deviations. For clarity only the best fit straight lines for the control observations are illustrated.

4. Discussion

We have examined the effects of β-adrenergic stimulation on the wild-type and ΔKPQ mutant sodium channel expressed in HEK cells. Prior studies of the adrenergic modulation of the human cardiac sodium channels were performed in frog oocytes. After preliminary experiments using both expression systems, we elected to use the mammalian cell line rather than the frog oocytes. Although current densities were at least as large as those in the oocyte, the much smaller size of the HEK cells permitted a more rapid voltage clamp. When the α-subunit of the sodium channel is expressed alone in the HEK cell, the sodium channel kinetics more closely resemble those in native cells. The availability of established cell lines and the presence of an endogenous adrenergic receptor are additional advantages of the HEK cells. In general, it was more difficult to obtain prolonged whole-cell recordings and cell-attached single-channel recordings in the HEK cells.

The gating kinetics of the sodium current were stable over the time required to complete the experiments reported here. In fact, we have observed stable activation and inactivation kinetics of the whole-cell sodium current for as much as one hour in the HEK cells. Native cells display a continuous shift in gating kinetics that would potentially confound the effects of adrenergic stimulation reported in the present study [42].

Isoproterenol and 8BcAMP shifted the voltage dependence of activation and inactivation to more negative potentials. The simultaneous shifts of both gating variables dictate that a complete assessment of the effect of adrenergic stimulation on the sodium current requires protocols that examine a range of membrane voltages. The shift in the voltage dependence of activation and inactivation were similar in hH1 and ΔKPQ. These results suggest any effect of adrenergic stimulation on sodium channel-dependent conduction variables would be similar for the two channel types.

The normal sodium channel may undergo inactivation from the closed or the open states. Both transitions are

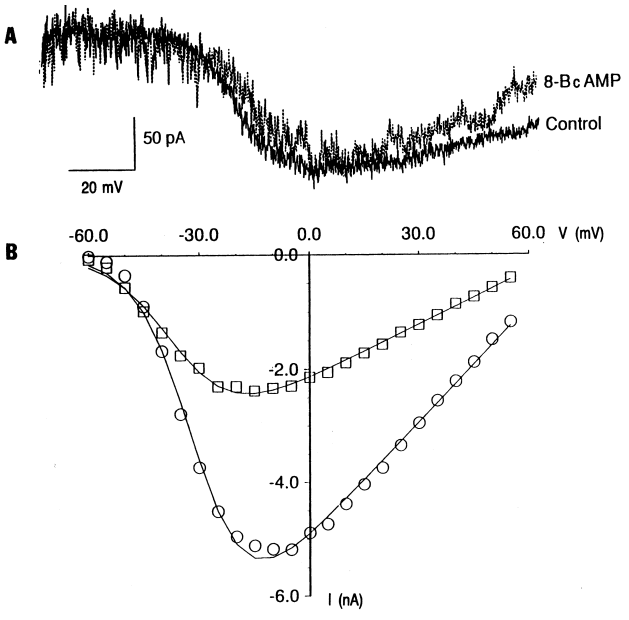

Fig. 10. Early and persistent currents in a cell expressing ΔKPQ. Panel A shows a leakage-subtracted whole-cell current obtained with a voltage ramp of 100 mV/s applied for 1.5 s (−100 to +50mV). Panel B shows the peak transient sodium current obtained during the control (circles) and exposure to 5 mM 8BcAMP (squares). Currents were elicited with 20-ms pulses from a holding potential of −100 mV.

absorbing. Closed state inactivation of the sodium channel shows greater voltage dependence than open state inactivation [48,49]. Deactivation and open state inactivation determine the mean open time of the sodium channel. Our results show that the greater steady-state inactivation during adrenergic stimulation results from faster closed-state inactivation. Mean open times were unaffected by adrenergic stimulation. We could not reduce the mean open times to the explicit inactivation and deactivation rate constants because of a number of confounding problems. We almost invariably had to use reduced holding potentials to partially inactivate a fraction of the channels. The theory of estimating the individual rate constants requires that the availability be one [50]. In the case of the ΔKPQ mutant, inactivation is no longer absorbing. This also confounds measurement of the individual rate constants.

At the depolarized potentials in the range of the plateau potential, β-adrenergic stimulation decreases the peak sodium current elicited from a holding potential of −100 mV because of an increase in steady-state inactivation. However, we did not observe a parallel decrease in the amplitude of the persistent sodium current in the ΔKPQ mutant channel. When expressed as a fraction of the peak current, the persistent current tended to increased. This result is consistent with the tentative conclusions about the nature of the persistent current. It results from intermittent failure of inactivation. Therefore a modulating influence which enhances inactivation may have no effect on the persistent sodium current

4.1. Comparison with prior studies of the cardiac and brain sodium channels

As there may be isoform differences in the modulation of the sodium channel by β-adrenergic stimulation, the most direct comparison can be made with studies of the cardiac sodium channel. Schreibmayer et al. examined the effect of β-adrenergic modulation of the rat cardiac sodium channel in frog oocytes [34]. Isoproterenol, cAMP and protein kinase A catalytic subunit all resulted in a 30% increase in sodium channel current, with no change in activation or inactivation gating. Mutation of all five strong PKA consensus phosphorylation sites did not change the effects of PKA stimulation. A similar study by Frohnwieser et al. using the human cardiac sodium channel expressed in frog oocytes observed a 42% increase in sodium conductance without a change in gating kinetics [51].

The differences in the results of those studies and those reported here may be related to the expression system. A similar divergence in the effect of PKA-dependent phosphorylation on the brain sodium channel expressed in mammalian cells and the frog oocyte has been reported [52,53]. Although the oocyte expression system has proved very effective for expressing a wide range of membrane proteins, translational processing may be different from that in mammalian cells. Therefore, the latter system may be preferable for the study of ion channel modulation.

A wide range of effects of β-adrenergic stimulation on the sodium current in native cell membranes has been reported. Because of the non-linear relationship between dV/dt max and the available sodium conductance, the early observations using these indirect approaches will not stand up to critical scrutiny [12,13,54]. However, the results using the direct sodium current measurement are not all in agreement. Conventional whole-cell voltage clamp experiments by Schubert et al., Ono et al and Gintant and Liu showed a shift in the voltage dependence of inactivation to more negative potential with β-adrenergic stimulation [14–16,55]. Using cell-attached recordings, Ono et al. showed that both the activation and inactivation voltage relationships were shifted to more negative potentials such that an increase or decrease in peak sodium current could be observed during β-adrenergic stimulation [17]. Our results are in agreement with the studies of Ono et al. showing a negative shift in both activation and inactivation voltage relationships. Qualitatively different results were obtained by Matsuda et al [56]. With β-adrenergic stimulation, they observed a voltage-dependent enhancement of the sodium current, an increase in the rate of inactivation but no change in steady-state inactivation. To be internally consistent, the rate of recovery from inactivation would also have to be increased. However, such data were not reported. The cardiac sodium channel in frog ventricular myocytes shows no regulation by β-adrenergic stimulation [57].

In the case of the brain sodium channel, there are also some inconsistencies in the published studies. The differences in results obtained with the oocyte and mammalian expression systems have been alluded to earlier. In mammalian expression systems, β-adrenergic stimulation reduced the sodium current by about 50% [52]. However, since no shift in the inactivation kinetics was observed, only a decrease in the number of functioning channels in the cell membrane can be reconciled with these results. Li et al. have shown that phosphorylation of serine 1506 in the III–IV linker by protein kinase C is required for the modulation of the brain sodium channel current by PKA [58].

We observed no evidence for a change in calcium to sodium permeability ratio of the human cardiac sodium channel expressed in HEK cells. Only the α-subunit was transfected into these cells. However, prior studies have shown relatively normal kinetics of the sodium channel expressed in mammalian cells [59,60]. The β-subunit influences on the level of channel expression and gating of the channel of the brain sodium channel [61–63]. For the cardiac sodium channel, Makita et al. reported that the β-subunit exerts no effect on the channel gating, whereas Nuss et al. reported an acceleration of macroscopic inactivation with α- and β-subunit co-expression. The basis for the differences in results is not clear as both groups used the frog oocyte expression system with similar voltage clamp protocols [64,65]. The high selectivity of the sodium channel for sodium over potassium and calcium ion is a function of the α subunit. Recent experiments suggest that a conserved motif 'DEKA', with each homologous domain contributing one member, regulates the cation selectivity of the sodium channel [66,67]. Converting residues K and A to E rendered the sodium channel calcium selective [68]. The lysine residue plays a critical role. The report by Santana et al. of an increase in calcium to sodium permeability during exposure to isoproterenol is an intriguing finding [18]. Concensus protein kinase A sites are remote from the pore and selectivity filter. Yet sympathetic stimulation results in a dramatic change in the calcium selectivity of the sodium channel. A number of factors may account for the differences between our results and those of Santana et al. The sodium and calcium currents were separated with tetrodotoxin and the organic calcium channel blocker nifedipine. A number of recent studies have demonstrated the presence of a tetrodotoxin-sensitive calcium current in cardiac myocytes [21,22]. Therefore, a shift in current reversal potential may result from a change in the relative size of multiple ion channel types with differing reversal potentials. β-adrenergic stimulation reverses the blocking action of the organic calcium channel blockers [24–26]. Our simpler recording system with a single transient inward current provides a direct way to test the sodium to calcium permeability ratio during β-adrenergic stimulation. Our results are not consistent with a greater calcium permeability during exposure to isoproterenol.

5. Clinical implication of the results

Our results suggest that β-adrenergic stimulation may alter the relative contribution of the persistent sodium current to the action potential during β-adrenergic stimulation. This may influence the action potential duration since the persistent current under basal conditions prolongs the QT interval. The implication to the susceptibility of arrhythmias in patients with the ΔKPQ-associated mutation will require the study of the effects of β-adrenergic stimulation on all the repolarizing currents, and the frequency dependence of the action potential duration. A recent study by Schwartz et al. of eight patients with sodium channel-associated (LQT3) and seven patients with potassium channel-associated (LQT2) mutations suggest some phenotypic differences [69]. Arrhythmias associated with the sodium channel mutation are more likely to occur during sleep rather than exercise. These observations would suggest a lesser role of β-adrenergic stimulation in the genesis of arrhythmias in LQT3. However, the authors cautioned, ''the limited sample size advises against extrapolation of these potentially important distinctions between LQT2 and LQT3 patients to the entire LQTS population.'' In fact, sympathetic activity may be increased intermittently during sleep. Exercise produced greater QTc shortening in patients with LQT3 compared to the control. This suggests some differences in the control of the action potential duration in LQT3. The general benefit of antiadrenergic treatment makes the study of the potential functional effects of β-adrenergic stimulation on all sodium channel-associated mutations important.

Acknowledgements

This work was supported by grant HL-32708 from the National Institutes of Health. Dr. Chauhan is a research fellow of the Heart and Stroke Foundation of Canada.

References

[1] Lown B, Verrier R. Neural activity and ventricular fibrillation. New Eng J Med 1976;294:1165–1170.
[2] Meredith IT, Broughton A, Jennings GL, Esler MD. Evidence of selective increase in cardiac sympathetic activity in patients with sustained ventricular tachycardia. New Eng J Med 1991;325:618–624.
[3] Steinbeck G, Andresen D, Bach P et al. A comparison of electrophysiologically guided antiarrhythmic drug therapy with beta-blocker therapy in patients with symptomatic sustained ventricular tachyarrhythmias. New Eng J Med 1992;327:987–992.
[4] Leenhardt A, Lucet V, Denjoy I et al. Catecholaminergic polymorphic ventricular tachycardia in children. Circulation 1995;91:1512–1519.
[5] Jervell A, Lange-Nielsen F. Congenital deaf-mutism, functional heart disease with prolongation of the Q–T interval, and sudden death. Am Heart J 1957;54:59–68.

[6] Ward OC. A new familial cardiac syndrome in children. J Irish Med Assoc 1964;54:103–106.
[7] Ramano C. Congenital Arrhythmia. Lancet 1965;26(ii):658–659.
[8] Jackman WC, Friday KJ, Anderson JL et al. The long QT syndromes: A critical review, new clinical observations and unifying hypothesis. Prog Cardiovasc Dis 1988;31:115–172.
[9] von Bernuth G, Belz GG, Evertz W, Stauch M. Qtu-abnormalities, sinus bradycardia and Adams-stokes attacks due to ventricular tachyarrhytmia. Acta Paediat Scand 1968;62:675–679.
[10] Shaw TRD. Recurrent ventricular fibrillation associated with normal QT intervals. Quarterly J Med, New Series L., No 200 1981:451–462.
[11] Schwartz PJ. Idiopathic long QT syndrome: Progress and questions. Am Heart J 1985;109:399–411.
[12] Windisch H, Tritthart HA. Isoproterenol, norepinephrine and phosphodiesterase inhibitors are blockers of the depressed fast Na^+-system in ventricular muscle fibers. J Mol Cell Cardiol 1982;14:431–434.
[13] Histome I, Kiyosue T, Imanishi S, Arita M. Isoproterenol inhibits residual fast channel via stimulation of β-adrenoceptors in guinea-pig ventricular muscle. J Mol Cell Cardiol 1985;17:657–665.
[14] Schubert B, VanDongen AMJ, Kirsh GE, Brown AM. β-adrenergic inhibition of cardiac sodium channels by dual G-protein pathways. Science 1989;245:516–519.
[15] Schubert B, VanDongen AMJ, Kirsh GE, Brown AM. Inhibition of cardiac Na^+ currents by isoproterenol. Am J Physiol 1990;258:H977–H982.
[16] Ono K, Kiyosue T, Arita M. Isoproterenol, DBcAMP and forskolin inhibit cardiac sodium current. Am J Physiol 1989;256:C1131–C1137.
[17] Ono K, Fozzard HA, Hanck D. On the mechanism of cAMP-dependent modulation of cardiac sodium channel current kinetics. Circ Res 1993;72:807–815.
[18] Santana LF, Gomez AM, Lederer WJ. Ca^{2+} flux through promiscuous cardiac Na^+ channels: Slip-mode conductance. Science 1998;279:1027–1033.
[19] Nilius B. Calcium block of guinea-pig heart sodium channels with and without modification by the piperazinylindole. J Physiol 1988;399:537–558.
[20] Sheets MF, Hanck DA. Mechanisms of extracellular divalent and trivalent cation block of the sodium current in canine cardiac Purkinje cells. J Physiol 1992;454:299–320.
[21] Lemaire S, Piot C, Seguin J, Nargeot J, Richard S. Tetrodotoxin-sensitive Ca^{2+} and Ba^{2+} currents in human atrial cells. Receptors and Channels 1995;3:71–81.
[22] Aggarwal R, Shorofsky SR, Goldman L, Balke CW. Tetrodotoxin-blockable calcium currents in rat ventricular myocytes; a third type of cardiac cell sodium current. J Physiol 1997;505(2):353–369.
[23] Cole WC, Chartier D, Martin M, Leblanc N. Ca^{2+} permeation through Na^+ channels in guinea pig ventricular myocytes. Am Heart J 1997;273:H128–H137.
[24] Grant AO, Katzung BG. The effects of quinidine and verapamil on electrically induced automaticity in the ventricular myocardium of guinea pig. J Pharmacol Exp Ther 1976;196:407–419.
[25] Legssyer A, Hove-Madsen L, Hoerter J, Fischmeister R. Sympathetic modulation of the effect of nifedipine on myocardial contraction and Ca current in the rat. J Mol Cell Cardiol 1997;29:579–591.
[26] McDonald T, Pelzer D, Trautwein W. Dual action (stimulation, inhibition) of D600 on contractility and calcium channels in guinea-pig and cat heart cells. J Physiol 1989;414:569–586.
[27] Gellens ME, George Jr. AL, Chen L et al. Primary structure and functional expression of the human cardiac tetrodotoxin-insensitive voltage-dependent sodium channel. Proc Natl Acad Sci 1992;89:554–558.
[28] Rogart RB, Cribbs LL, Muglia LK, Kephart DD, Kaiser MW. Molecular cloning of a putative tetrodotoxin-resistant rat heart Na^+ channel isoform. Proc Natl Acad Sci 1989;86:8170–8174.
[29] Wang Q, Shen J, Li Z et al. Cardiac sodium channel mutations in patients with long QT syndrome, an inherited cardiac arrhythmia. Human Molec Genetics 1995;4:1603–1607.
[30] Wang Q, Shen J, Splawski I et al. SCN5A mutations associated with an inherited cardiac arrhythmia, long QT syndrome. Cell 1995;80:805–811.
[31] Bennett PB, Yazawa K, Makita N, George Jr. AL. Molecular mechanism for an inherited cardiac arrhythmia. Nature 1995;376:683–685.
[32] Dumaine R, Wang Q, Keating MT et al. Multiple mechanisms of Na^+ channel-linked long-QT syndrome. Circ Res 1996;78:916–924.
[33] An R-H, Bangalore R, Kass RS. Lidocaine block of LQT-3 mutant human Na^+ channels. Circ Res 1996;79:103–108.
[34] Schreibmayer W, Frohnwieser B, Dascal N et al. β-adrenergic modulation of currents produced by Rat cardiac Na+ channels expressed in *Xenopus laevis* oocytes. Receptors and Channels 1994;2:339–350.
[35] Freedman NJ, Liggett SB, Drachman DE et al. Phosphorylation and desensitization of the human β_1-adrenergic receptor. J Biol Chem 1995;270:17953–17961.
[36] Chandra R, Starmer CF, Grant AO. Multiple effects of the KPQ deletion mutation on the gating of human cardiac sodium channels expressed in mammalian cells. Am J Physiol 1998;274:H1643–H1654.
[37] Zhu G, Zhang Y, Xu H, Jiang C. Identification of endogenous outward currents in the human embryonic kidney (HEK293) cell line. J Neurosci Methods 1998;81:73–83.
[38] Gilliam FR III, Starmer CF, Grant AO. Blockade of rabbit atrial sodium channels by lidocaine: Characterization of continuous and frequency-dependent blocking. Circ Res 1989;65:723–739.
[39] Grant AO, Starmer CF. Mechanisms of closure of cardiac sodium channels in rabbit ventricular myocytes: Single-channel analysis. Circ Res 1987;60:897–913.
[40] Hurwitz JL, Dietz MA, Starmer CF, Grant OA. Source of bias in the analysis of single-channel data: Assessing the apparent interaction between channel proteins. Computers Biomedial Res 1991;24:584–602.
[41] Fozzard H, Hanck DA. Structure and function of voltage-dependent sodium channels: Comparison of brain II and cardiac isoforms. Physiol Rev 1996;76:887–926.
[42] Hanck DA, Sheets MF. Time-dependent changes in the kinetics of sodium current in single canine cardiac Purkinje cells. Am J Physiol 1992;262:H1197–H1207.
[43] Hille B. In: Ionic channels of excitable membranes, Sinauer Associates, Inc, Sunderland, 1984, pp. 249–271.
[44] Fernandez JM, Fox AP, Krasne G. Membrane patches and whole-cell membranes: A comparison of electrical properties in rat clonal pituitary (GH3) cells. J Physiol 1984;356:565–585.
[45] Fatt P, Ginsborg BL. The ionic requirements for the production of action potentials in crustacean muscle fibres. J Physiol 1958;142:516–543.
[46] Dudel J, Peper K, Rudel R, Trautwein W. The effect of tetrodotoxin on the membrane current in cardiac muscle (Purkinje fibers). Pflugers Arch 1967;295:213–226.
[47] Wang DW, Yazawa K, George Jr. AL, Bennett PB. Characterization of human cardiac Na^+ channel mutations in the congenital long QT syndrome. Proc Natl Acad Sci 1996;93:13200–13205.
[48] Aldrich RW, Stevens CF. Voltage-dependent gating of single sodium channels from mammalian neuroblastoma cells. J Neurosci 1987;7:418–431.
[49] Yue DT, Lawrence JH, Marban E. Two molecular transitions influence cardiac sodium channel gating. Science 1989;244:349–352.
[50] Aldrich RW, Stevens CF. Inactivation of open and closed sodium channels determined separately. Symposia on Quantitative Biol 1983;47:147–153.
[51] Frohnwieser B, Chen L-Q, Schreibmayer W, Kallen RG. Modulation of the human cardiac sodium channel α-subunit by cAMP-dependent protein kinase and the responsible sequence domain. J Physiol 1997;498:309–318.

[52] Li M, West JW, Lai Y, Scheuer T, Catterall WA. Functional modulation of brain sodium channels by cAMP-dependent phosphorylation. Neuron 1992;8:1151–1159.
[53] Smith RD, Goldin AL. Protein kinase A phosphorylation enhances sodium channel currents in *Xenopus* oocytes. Am J Physiol 1992;263:C660–C666.
[54] Gillis AM, Kohlhardt M. Voltage-dependent V_{max} blockade in Na^+-dependent action potentials after β_1 and H_2-receptor stimulation in mammalian ventricular myocardium. Can J Physiol 1988;66:1291–1296.
[55] Gintant GA, Liu D-W. β-adrenergic modulation of fast inward sodium current in canine myocardium syncytial preparations versus isolated myocytes. Circ Res 1992;70:844–850.
[56] Matsuda JJ, Lee H, Shibata EF. Enhancement of rabbit cardiac sodium channels by β-adrenergic stimulation. Circ Res 1992;70:199–207.
[57] Sumii K, Munemori M, Miyoshi H, Seyama I. Intracellular signal transduction systems do not regulate Na channel in from ventricular cells. Am J Physiol 1994;267:H563–H568.
[58] Li M, West JW, Numann R, Murphy FJ, Scheuer T, Catterall WA. Convergent regulation of sodium channels by protein kinase C and cAMP-dependent protein kinase. Science 1993;261:1439–1442.
[59] Scheuer T, Auld VJ, Boyd S et al. Functional properties of rat brain sodium channels expressed in a somatic cell line. Science 1990;447:854–858.
[60] Ukomadu C, Zhou J, Sigworth FJ, Agnew WS. ml Na^+ channels expressed transiently in human embryonic kidney cells: Biochemical and biophysical properties. Neuron 1992;8:663–676.
[61] Isom LL, De Jongh KS, Patton DE et al. Primary structure and functional expression of the β_1 subunit of the rat brain sodium channel. Science 1992;256:839–842.
[62] Isom LL, Scheuer T, Brownstein AB et al. Function co-expression of the β1 and type IIA a subunits of sodium channels in a mammalian cell line. J Biol Chem 1995;270:3306–3312.
[63] Makita N, Bennett Jr. PB, George Jr. AL. Voltage-gated Na^+ channel β1 subunit mRNA expressed in adult human skeletal muscle heart and brain is encoded by a single gene. J Biol Chem 1994;269:7571–7578.
[64] Makita N, Bennett Jr. PB, George Jr. AL. Voltage-gated Na^+ channel β1 subunit mRNA expressed in adult human skeletal muscle, heart and brain is encoded by a single gene. J Biol Chem 1994;269:7571–7578.
[65] Nuss HB, Chiamvimonvat N, Perez-Garcia MT, Tomaselli GF, Marban E. Functional association of the β1 subunit with human cardiac (hH1) and rat skeletal muscle (μl) sodium channel a subunits expressed in *Xenopus* oocytes. J Gen Physiol 1995;106:1171–1191.
[66] Favre I, Moczydlowski E, Schild L. On the structural basis for ionic selectivity among Na^+, K^+ and Ca^{2+} in the voltage-gated sodium channel. Biophys J 1996;71:3110–3125.
[67] Perez-Garcia MT, Chiamvimonvat N, Ranjan R et al. Mechanisms of sodium/calcium selectivity in sodium channels probed by cysteine mutagenesis and sulfhydryl modification. Biophys J 1997;71:989–996.
[68] Heinemann SH, Terlau H, Stuhmer W, Imoto K, Numa S. Calcium channel characteristics conferred on the sodium channel by single mutations. Nature 1992;356:441–443.
[69] Schwartz PJ, Priora SG, Locati EH et al. Long QT syndrome patients with mutations of the SCN5A and HERG genes have differential responses to Na^+ channel blockade and to increases in heart rate. Circulation 1995;92:3381–3386.